Electronic Supplementary Material (ESI) for Polymer Chemistry.

SUPPORTING INFORMATION

Design of Thiol- and Light-sensitive Degradable Hydrogels using Michael-type Addition Reactions

Prathamesh M. Kharkar,[a] Kristi L. Kiick,[*abc] and April M. Kloxin,*[ad]

[a]Department of Materials Science and Engineering, University of Delaware, Newark, DE 19716, USA. E-mail: kiick@udel.edu; akloxin@udel.edu;

[b]Department of Biomedical Engineering, University of Delaware, Newark, DE 19716, USA

[c]Delaware Biotechnology Institute, University of Delaware, Newark, DE 19716, USA

[d]Department of Chemical and Biomolecular Engineering, University of Delaware, Newark, DE 19716, USA

Table of contents

1. Materials

General organic reagents and solvents were purchased from commercial sources and used as received unless otherwise stated. Four-arm poly(ethylene glycol) (PEG, 10 000 g mol^{-1}) with hydroxyl, thiol, or amine end groups was obtained from JenKem Technology USA (Allen, TX). Deionized water (18 MΩ-cm) was used for experimental procedures.

2. Organic Synthesis and polymer modification

All reactions were conducted in glassware that was oven-dried and cooled under argon. All reactions were performed at least in duplicate and under an inert argon atmosphere using a Schlenk line unless noted otherwise. Chromatography was performed on silica gel (Sorbent Technologies, 40-63 µm, 60 Å). ^{1}H spectra were recorded using a Bruker NMR spectrometer (Bruker Daltonics, Billerica, MA) under standard quantitative conditions (600 Hz, 128 scans).

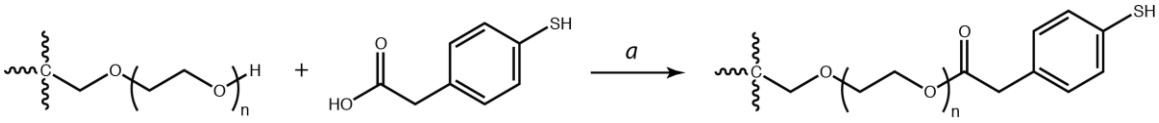

Scheme S1. Synthesis of PEG-MPA. 4-arm PEG was reacted with 4-mercaptophenylacetic acid (MPA) to yield aryl thiol end-functionalized PEG (a: Toluene, PTSA, ~110 ^{0}C)

*Mercaptophenylacetic acid based aryl thiol-end functionalized PEG (**PEG-MPA**)*

PEG was modified with 4-mercaptophenylacetic acid (MPA) based on a modified version of a previously published protocol.[2] Briefly, hydroxyl end-functionalized 4-arm PEG (1 g, 0.1 mmol), MPA (0.67 g, 4 mmol), and *p*-toluenesulfonic acid (0.07 g, 0.04 mmol) were dissolved in toluene (20 mL) and refluxed at 110 ^{0}C for 48 hours. The reaction was subsequently precipitated in ethyl ether (50 mL, 4 ^{0}C), and polymer was recovered by filtration. The polymer was washed with isopropanol and hexane and further reduced using dithiothreitol (DTT). The product was dissolved in methanol, filtered through a 0.22-µm filter, and precipitated in isopropanol. The final dried polymer (0.5 g, 66% yield) was obtained by removal of residual solvents under reduced pressure at room temperature.

^{1}H NMR (400 MHz, Chloroform) δ: 7.24–7.08(m, 16H), 4.24 (t, 8H), 3.90–3.35 (bs, 900H), 3.42–3.39 (s, 4H).

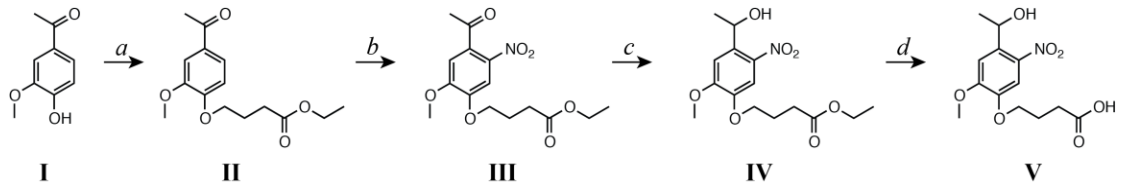

Scheme S2. Synthetic route for preparing small molecule photolabile precursor. Reagents and conditions are as follows: ***a)*** ethyl-4-bromobutyrate, potassium carbonate in DMF; ***b)*** nitric acid (69.3% w/w); ***c)*** sodium borohydride in ethanol at 38 ^{0}C; and ***d)***, potassium hydroxide in water:THF (1:1). Each chemical compound is numbered for its identification in experimental procedures.

*Ethyl 4-(4-acetyl-2-methoxyphenoxy)butanoate (**II**)*

Synthesis of intermediate **II** to **V** was based on a modified version of a previously published protocol.[1] Briefly, 1-(4-hydroxy-3-methoxyphenyl)ethanone (**I**, 30 g, 180.5 mmol), ethyl-4-bromobutyrate (31 mL, 217 mmol), and potassium carbonate (37.4 g, 271 mmol) were added to DMF (150 mL) and stirred overnight under argon. The reaction mixture was precipitated into DI water (2000 mL), stirred for 2 hours, and stored overnight at 4 ^{0}C for maximum precipitation. The resulting precipitant was filtered and washed with a copious amount of water. The product was subsequently dried at room temperature in a vacuum oven, and the final product was collected as a white powder (47.4 g, 94%).

^{1}H NMR (600 MHz, Chloroform) δ 7.61 – 7.46 (m, 2H), 6.87 (d, 1H), 4.16 – 4.09 (m, 4H), 3.89 (s, 3H), 2.56 – 2.50 (m, 5H), 2.20 – 2.14 (m, 2H), 1.24 (t, 3H).

*Ethyl 4-(4-acetyl-2-methoxy-5-nitrophenoxy)butanoate (**III**)*

Ethyl 4-(4-acetyl-2-methoxyphenoxy)butanoate (**II**, 25 g, 87.6 mmol) was added slowly to nitric acid (70 mL, 4 ^{0}C, ice bath) over the period of 1 hour using small portions while monitoring the reaction temperature to ensure it remained below 30 ^{0}C. The reaction was allowed to proceed on an ice bath for approximately 30 minutes until completion as assessed by thin-layer chromatography (TLC) (50:50 ethyl acetate:hexane, product r_f ~0.5). The reaction mixture was precipitated in DI water (1000 mL), stirred for 2 hours, and stored overnight at 4 ^{0}C for maximum precipitation. The yellow solid precipitate that was obtained after filtration was further purified by recrystallization in ethanol (300 mL, 78 ^{0}C). Purification using flash chromatography (3:7 ethyl acetate:hexane to 6:4 ethyl acetate:hexane) yielded the yellow solid product (21.2 g, 73%).

^{1}H NMR (600 MHz, DMSO) δ 7.61 (s, 1H), 7.21 (s, 1H), 4.13 – 4.03 (m, 4H), 3.92 (s, 3H), 2.44 (t, 2H), 1.99 (t, 2H), 1.17 (t, 3H).

*Ethyl 4-(4-(1-hydroxyethyl)-2-methoxy-5-nitrophenoxy)butanoate (**IV**)*

Ethyl 4-(4-acetyl-2-methoxy-5-nitrophenoxy)butanoate (**III**, 18 g, 55 mmol) was dissolved in ethanol (200 mL), and sodium borohydride (1.3 g, 35 mmol) was slowly added to the reaction mixture. The reaction was allowed to proceed at 38 ^{0}C overnight.

The reaction mixture was precipitated in DI water (3000 mL), stirred for 2 hours, and stored overnight at 4 ^{0}C for maximum precipitation. The resultant precipitant was filtered and washed with water to collect the product (11.6 g, 64%) as a pale yellow powder.
^{1}H NMR (600 MHz, DMSO) δ 7.52 (s, 1H), 7.36 (s, 1H), 5.47 (s, 1H), 5.25 (d, 1H), 4.06 (q, 4H), 3.90 (s, 3H), 2.45 (t, 2H), 2.08 – 1.91 (m, 2H), 1.36 (d, 3H), 1.18 (t, 3H).

*4-(4-(1-hydroxyethyl)-2-methoxy-5-nitrophenoxy)butanoic acid (**V**)*
Ethyl 4-(4-(1-hydroxyethyl)-2-methoxy-5-nitrophenoxy)butanoate (**IV**, 10 g, 31 mmol) and potassium hydroxide (2.5 g, 44 mmol) were added to a solution of 1:1 THF (100 mL) and water (100 mL) for ester cleavage. The reaction mixture was stirred at room temperature for 2 hours. The pH of the reaction mixture was dropped to ~4 using hydrochloric acid until precipitant formation. The resulting mixture was stored overnight at 4 ^{0}C, and product (7.7 g, 72%) was recovered using filtration and dried using a vacuum oven at 40 ^{0}C.
^{1}H NMR (600 MHz, DMSO) δ 12.16 (s, 1H), 7.53 (s, 1H), 7.36 (s, 1H), 5.56 – 5.38 (m, 1H), 5.25 (q, 1H), 4.05 (t, 2H), 3.90 (s, 3H), 2.39 (t, 2H), 1.95 (p, 2H), 1.37 (d, 3H).

*Hydroxyl end-functionalized photodegradable PEG intermediate (**pII**)*
4-(4-(1-hydroxyethyl)-2-methoxy-5-nitrophenoxy)butanoic acid (**V**, 0.12 g, 0.4 mmol) was dissolved in DMF (10 mL). HATU (0.15 g, 0.4 mmol), DIEA (0.10 g, 0.8 mmol), and amine end-functionalized 4-arm PEG (***p*I**, 0.5 g, 0.05 mmol) were added to the reaction, and the reaction was allowed to proceed overnight at room temperature. The reaction was subsequently precipitated in ethyl ether (100 mL, 4 ^{0}C), and the polymer was recovered by filtration. The final dried polymer product was obtained by removal of residual solvents under reduced pressure. The dry polymer was dissolved in water (~20 mL), dialyzed (MWCO 2000 g/mol, against 3.5 liter of DI water with a total of 6 changes over 48 hours at room temperature), and then lyophilized to give a yellow solid (0.45 g, 82%).
^{1}H NMR (600 MHz, DMSO) δ 7.91 (t, 4H), 7.52 (s, 4H), 7.36 (s, 4H), 5.46 (d, 4H), 5.26 (qd, 4H), 4.03 (td, 8H), 3.90 (s, 12H), 3.75 – 3.35 (bs, 900H), 2.25 (t, 8H), 1.94 (p, 8H), 1.36 (d, 12H).

*Carboxyl end-functionalized photodegradable PEG intermediate (**pIII**)*
Hydroxy end-functionalized photodegradable PEG intermediate (***p*II**, 0.5 g, 0.04 mmol), succinic anhydride (0.14 g, 1.4 mmol), and DMAP (0.08 g, 0.71 mmol) were dissolved in DMF (1.5 mL) and heated to 50 ^{0}C overnight. The reaction mixture was subsequently precipitated in ethyl ether (50 mL, 4 ^{0}C), and the polymer was recovered by filtration. The final dried polymer was obtained by removal of residual solvents under reduced pressure. The filtered polymer was dissolved in water, dialyzed (MWCO 2000 g/mol,

against 3.5 liter of DI water with a total of 6 changes over 48 hours at room temperature), and then lyophilized to give a dark orange solid (0.41 g, 79%).
^{1}H NMR (600 MHz, DMSO) δ 7.92 (t, 4H), 7.55 (s, 4H), 7.10 (d, 4H), 6.17 (q, 4H), 4.04 (t, 8H), 3.95 (d, 12H), 3.75 – 3.35 (bs, 900H), 2.54 (td, 8H), 2.44 (t, 8H), 2.24 (t, 8H), 1.94 (h, 8H), 1.56 (d, 12H).

*Maleimide end-functionalized photodegradable PEG (**pIV**)*
Carboxy end-functionalized photodegradable PEG intermediate (**pIII**, 0.5 g, 0.04 mmol), N-(2-aminoethyl) maleimide (0.08 g, 0.34 mmol), HATU (0.09 g, 0.26 mmol), and DIPEA (0.04 g, 0.34 mmol) were dissolved in DMF (5 mL) and reacted overnight at room temperature. The reaction was subsequently precipitated in ethyl ether (50 mL, 4 ^{0}C), and the polymer was recovered by filtration. The final dried polymer was obtained by removal of residual solvents under reduced pressure. The filtered polymer was dissolved in water, dialyzed (MWCO 2000 g/mol, against 3.5 liter of DI water with a total of 6 changes over 48 hours at room temperature), and then lyophilized to give a dark orange solid (0.46 g, 82%).
^{1}H NMR (600 MHz, DMSO) δ 7.94 (dt, 8H), 7.55 (s, 4H), 7.09 (s, 4H), 6.97 (d, 8H), 6.16 (q, 4H), 4.04 (t, 8H), 3.96 (s, 12H), 3.75 – 3.35 (bs, 900H), 2.25 (t, 12H), 1.94 (h, 8H), 1.54 (d, 12H).

3. Hydrogel formation and rheological characterization

Thiol and maleimide based PEG precursor solutions were prepared individually in citric acid (pH 3, prepared using citric acid and disodium phosphate) and phosphate buffered saline (pH 7.4), respectively. Hydrogels were formed by vortex mixing the macromolecular precursor solutions at 1:1 stoichiometric ratio (maleimide:aryl thiol). Reaction at acidic pH allowed additional time for vortex mixing before gelation occurred, resulting in homogeneous hydrogels. For rheological and mechanical characterization, oscillatory rheology experiments were conducted on a stress-controlled AR-G2 rheometer (TA Instruments). Hydrogels were formed directly on a Peltier plate pre-cooled to 4 ^{0}C. Gelation at reduced temperature allowed sufficient time to lower the parallel plate geometry to the geometry gap (120 μm) before onset of gelation. Time sweep measurements (1% constant strain and 6 rad/s frequency) were obtained under the viscoelastic regime to obtain gelation kinetics and final shear modulus of the hydrogels (**Fig. S1**). The final shear modulus was defined as the modulus value after reaching the plateau region. The crosslinking time was defined as the time to reach 90% of the final modulus.

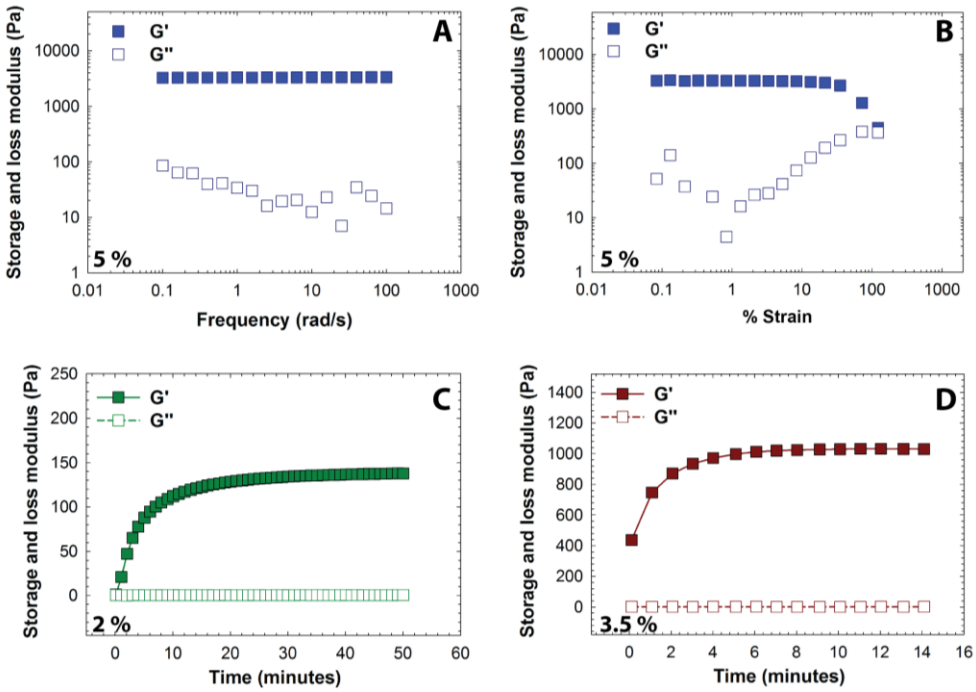

Fig. S1. Rheological characterization under the linear viscoelastic regime. (**A**) Frequency and (**B**) strain sweep data was used to determine the linear viscoelastic regime for subsequent rheological characterization (representative data for a 5 wt% gel sample shown). Representative dynamic time sweep measurements for (**C**) 2 wt% and (**D**) 3.5 wt% are shown.

Table S1. Mechanical properties of hydrogels

Polymer Concentration	Swelling ratio	Storage modulus *(Pa)*	Crosslinking time *(min)*
2 weight %	32.1 ± 2.7	222.9 ± 47.9	10.4 ± 2.9
3.5 weight %	25.9 ± 0.3	1277.0 ± 173.9	2.8 ± 0.2
5 weight %	17.1 ± 0.9	3584.9 ± 421.3	2.4 ± 0.4

4. Mesh size calculations

The mesh size of the hydrogels was calculated based on previously published protocols.[2, 3] Briefly, the Flory-Rehner equation was used to obtain the average molecular weight between crosslinks ($\overline{M_c}$) as shown below.[3, 4]

$$\frac{1}{\overline{M_c}} = \frac{2}{\overline{M_n}} - \frac{(\bar{v}/V_1)(\ln(1-v_2) + v_2 + \chi_1 v_2^2)}{v_2^{1/3} - (v_2/2)} \quad \ldots(S1)$$

where $\overline{M_n}$ is the number average molecular weight of the uncrosslinked macromolecular chain; $\bar{v}$ is the specific volume of the polymer; $V_1$is the molar volume of the solvent (18 cm^3/mol for water); v_2 is the equilibrium volume fraction ($v_2 = Q^{-1}$, measured in PBS); and χ_1 is the polymer-solvent interaction parameter (0.45 for PEG-water solutions).[5] Subsequently, the unperturbed root-mean-square end-to-end distance ($(\bar{r}_0^2)^{1/2}$) was calculated using following equation:

$$(\bar{r}_0^2)^{1/2} = lC_n^{1/2}\left(\frac{2\overline{M_c}}{M_r}\right)^{1/2} \quad \ldots(S2)$$

where l represents the average bond length (1.46 Å); C_n is the characteristic ratio for PEG, taken here as 4; and M_r is the molecular weight of the polymer repeat unit (44 g/mol for PEG). The mesh size was calculated using the following equation for 2%, 3.5% and 5% hydrogel compositions (**Fig. S2**)[6]

$$\xi = v_2^{-1/3}(\bar{r}_0^2)^{1/2} \quad \ldots(S3)$$

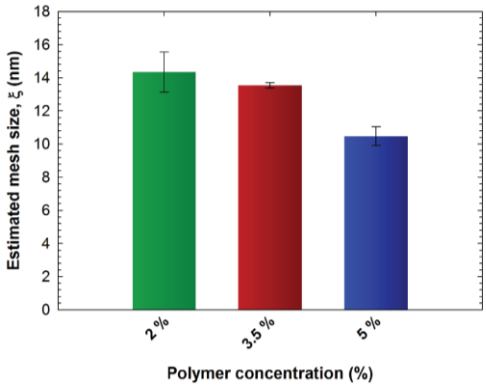

Fig. S2. Influence of polymer concentration on PEG hydrogel mesh size. Estimated value of the mesh size decreased with increase in the polymer concentration, which can be attributed to the resulting increase in the crosslink density per the theory of rubber elasticity. The data shown illustrate the mean (n ≥ 3) with error bars showing the standard error.

5. Absorbance of photodegradable PEG macromonomer

The absorbance of maleimide end-functionalized photodegradable PEG (*pIV*) was measured using a UV-visible spectrophotometer (NanoDrop 2000C, Thermo Fisher Scientific) at 10 mg/mL in PBS buffer (**Fig. S3**). The molar absorptivity was calculated using the Beer-Lambert law

$$A = abc \quad \ldots(S4)$$

where A represents the absorption, a is the molar absorptivity; b is the path length (1 mm); and c is the concentration of photodegradable moiety (2 x 10^{-3} mol/L).

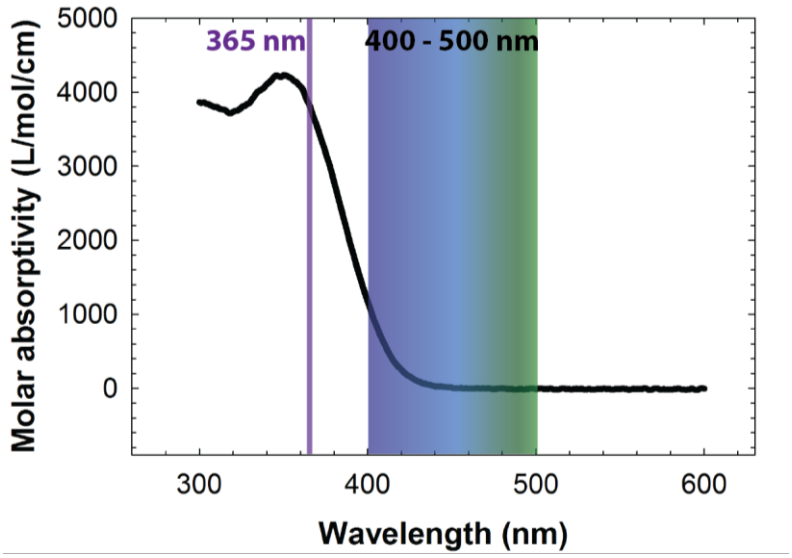

Fig. S3. Molar absorptivity of the photolabile moiety on the photodegradable macromer. The nitrobenzyl ether based photolabile moiety absorbs 365 nm UV light strongly compared to 400 to 500 nm visible light wavelengths.

6. Degradation monitored using oscillatory rheometery

For characterization of photodegradation, the hydrogels were directly formed on the rheometer plate; after gelation was complete, low doses of light were applied (10 mW cm^{-2} at 365 nm [long wavelength UV] or 400-500 nm [visible], Exfo Omnicure Series 2000 light source with appropriate bandpass filter, SilverLine UV or International Light Radiometer). For the step-wise degradation study, 30 seconds of light were applied every 5 minutes, whereas for the continuous degradation study, light was constantly applied (<5 minutes for 365 nm and ~60 minutes for 400 to 500 nm wavelength). The degradation was monitored using time sweep measurements in the linear viscoelastic regime (1% constant strain and 6 rad/s frequency). Hydrogels prepared using 4-arm maleimide end-functionalized PEG (without photodegradable groups) and 4-arm PEG-alkylSH served as a negative (nondegradable) control for photodegradation studies (**Fig. S4**).

For GSH-mediated degradation and hydrolytic degradation, hydrogel discs (diameter = 4.6 mm, thickness = 1.8 mm) were prepared by mixing macromolecular precursor solutions (5% w/w) in a 1:1 maleimide:thiol molar ratio and allowing individual hydrogel formation within a cylindrical mold (30 μL of solution into a 1-mL syringe with tip removed). The resulting hydrogels subsequently were washed with PBS and incubated in appropriate degradation stimuli (10 mM GSH for GSH-mediated degradation and PBS for hydrolytic degradation, pH 7.4) at room temperature. Degradation was monitored

using shear moduli measurements (2 rad/s, 2% strain, and 0.25 N normal force to prevent hydrogel slip). Hydrogels prepared using 4-arm maleimide end-functionalized PEG (without the photodegradable group) and 4-arm alkyl thiol end-functionalized PEG served as a negative (nondegradable) control for GSH-mediated and hydrolytic degradation experiments. The 5 wt% composition was chosen for studying the degradation rates and cargo release of these multimodal hydrogels owing to the ease of handling the higher-modulus formulation relative to the lower moduli 2 and 3 wt% gels.

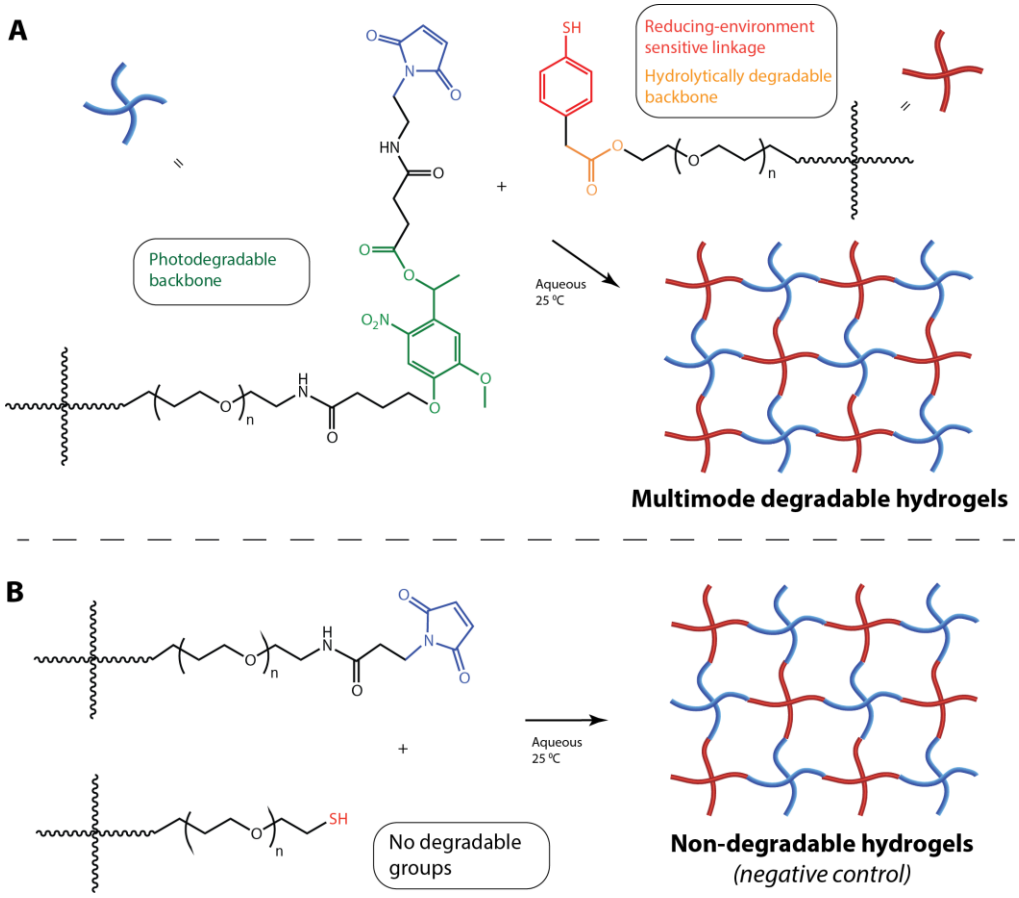

Fig. S4. Structural differences between the (A) multimode degradable and (B) nondegradable negative control hydrogels. Nondegradable hydrogels (negative control) were prepared by reacting maleimide end functionalized PEG with the alkyl thiol end-functionalized four-arm PEG. The resulting hydrogels thus did not contain any degradable or chemically susceptible functional groups within the backbone structure, as compared with multimode degradable hydrogels.

7. Degradation Kinetics

For calculating degradation kinetics, hydrogel modulus was monitored as a function of time in response to appropriate degradation stimuli. Hydrogel modulus can be expressed in terms of the molecular weight between the crosslinks for the equilibrium swollen gel

(M_c) and the volumetric swelling ratio (Q) per the theory of rubber elasticity, as shown in the following equation.[7]

$$G = \frac{\rho RT}{M_c} Q^{-1/3} = \rho_x RT Q^{-1/3}$$

…*(S5)*

where ρ is the density of the polymer; R is the universal gas constant; T is the temperature; and ρ_x is the crosslink density. Based on the network connectivity, we assume that the cleavage of the labile linkages (DL = degradable linkages) will dictate the rate of degradation of the hydrogel, and consequently, the rate equation can be expressed in first order kinetics as shown below (pseudo-first order for ester hydrolysis and reversible click and thiol exchange where water and GSH, respectively, are in great excess).

$$-\frac{d[DL]}{dt} = k\,[DL]$$

…*(S6)*

where [DL] represents the concentration of degradable linkages within the multimode degradable hydrogels, and k represents the first order degradation rate constant. Integration of equation S6 from time 0 to t and concentration of degradable crosslinks from $[DL]_0$ to [DL] results in the following equation.

$$[DL] = [DL]_0\, e^{-k_{eff}t}$$

…*(S7)*

Since the degradable linkages are directly correlated to the crosslink density (ρ_x) for these hydrogels, we arrive at equation S8 based on equation S5 and S7, as shown below.

$$G \propto \rho_x \propto e^{-k_{eff}t}$$

…*(S8)*

Using this generalization, the rate constants for various modes of degradation were calculated (**Table 1**). The regression analysis for all three modes of degradation for early time points is shown in **Fig. S5**.

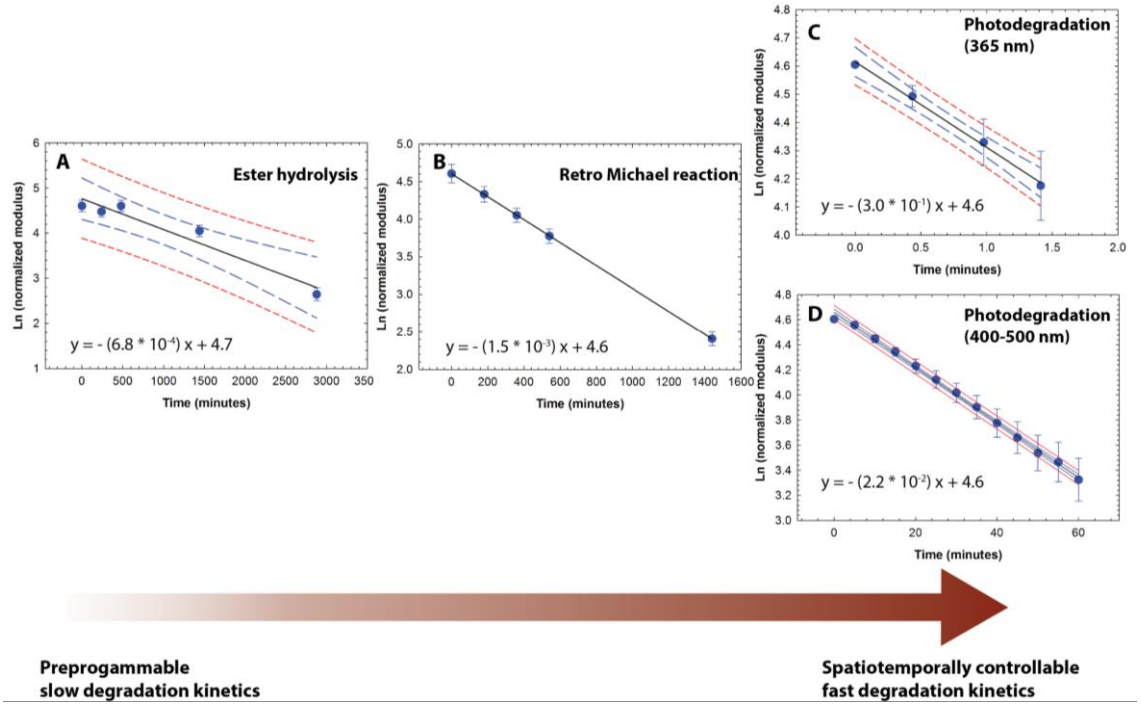

Fig. S5. Regression analysis for degradation of multimode degradable hydrogels. Multimode degradable hydrogels exhibited first order degradation kinetics in response to the (**A**) aqueous microenvironment (PBS buffer) with a rate constant of 6.84 x 10^{-4} min^{-1}, (**B**) reducing microenvironment (10 mM GSH) with a rate constant of 1.56 x 10^{-3} min^{-1}, and applied light (10 mW/cm^2) at (**C**) 365 nm with a rate constant of 3.03 x 10^{-1} min^{-1} and (**D**) 400 to 500 nm with a rate constant of 2.20 x 10^{-2} min^{-1}. The data shown illustrate the mean ($n \geq 3$) with error bars showing the standard error. The black line indicates the linear fit using regression analysis. Blue (long dashes) and red lines (short dashes) indicate 95% confidence and prediction intervals, respectively.

8. Degradation monitored using hydrogel volume

Hydrogel discs (diameter ~4.6 mm and thickness ~1.8 mm) were incubated in appropriate degradation microenvironment at room temperature. At predefined time points, the hydrogel discs were removed; the diameter of the sample was measured using a Vernier caliper; and the height of the sample was measured using the rheometer gap values (parallel plate geometry). The volume of the hydrogel was calculated at each time point assuming an ideal cylindrical geometry. The hydrogel volume at each time point was normalized to the initial volume at time t = 0 for that gel composition (**Fig. S6**).

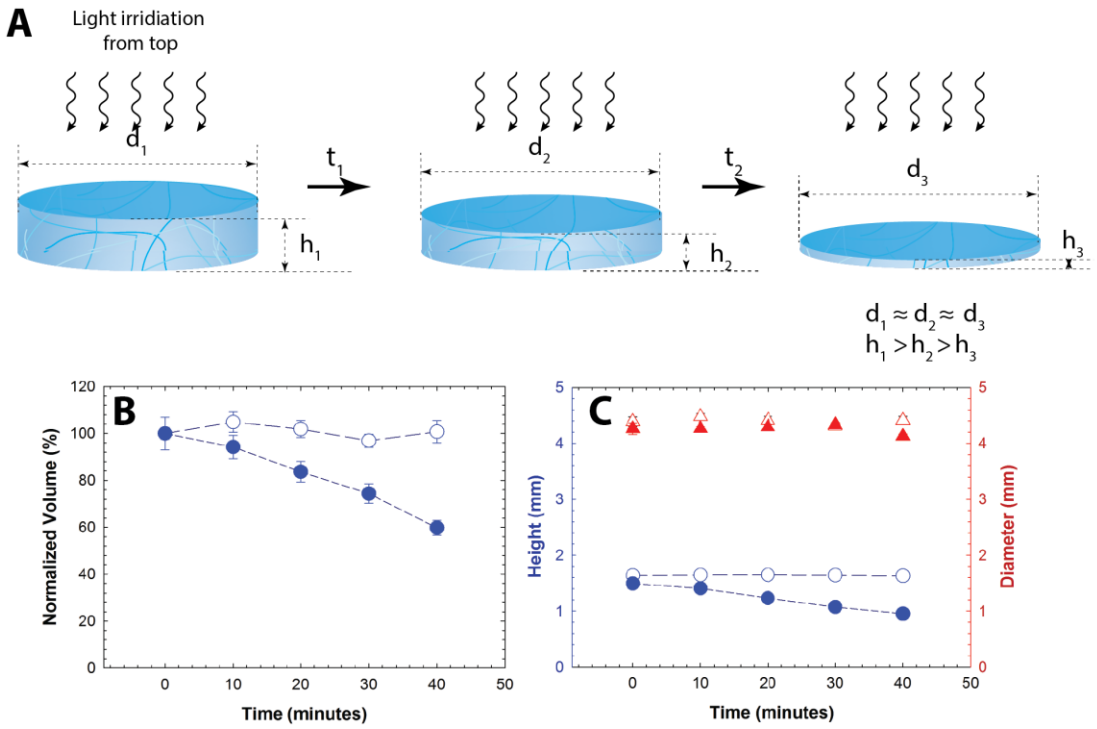

Fig. S6. Light-mediated surface erosion of hydrogels. (**A**) Schematic showing surface erosion of the hydrogel upon application of light (10 mW/cm^2 at 365 nm). (**B**) Multimode degradable hydrogels exhibit a continuous decrease in the normalized volume (closed circle symbols) compared with the negative control (open circle symbols), indicating surface erosion due to degradation of the hydrogel with continuous externally-applied light. The changes in volume are associated with (**C**) the changes in the height of hydrogel samples, where a continuous decrease in the height with limited changes in diameter are observed, suggesting surface erosion is the prominent mode of degradation of the multimode hydrogel samples upon irradiation (open symbols = negative control and closed symbols = multimode degradable gels; triangle = diameter; circles = height). The data shown illustrate the mean ($n \geq 3$) with error bars showing the standard error.

9. Calculating light attenuation

Percent transmittance was calculated using the Beer-Lambert law as shown below,

$$A = \frac{log_{10}100}{\%\,T} = abc \qquad \ldots(S9)$$

where A represents absorbance; $\%\,T$ is the percentage of transmitted light; a is the molar absorptivity of the photolabile group (3840 L mol^{-1} cm^{-1} at 365 nm); b is the pathlength (depth of penetration); and c is the concentration of photodegradable moiety present in the 5 wt % hydrogel (8.3 x 10^{-3} mol/L). With this, approximately 6% of incident light is estimated to penetrate 100-µm deep into these thick hydrogels resulting in surface erosion of the hydrogel.

10. Cargo release

Fluorescently labeled polymeric nanobeads (mean particle size = 100 nm, Em = 481 nm, Ex = 644 nm, 16.67 % v/v) were mixed with the maleimide-functionalized macromolecular precursor solution. The photodegradable maleimide and aryl thiol end-functionalized macromolecular precursors were subsequently mixed at 1:1 stoichiometry to yield homogeneous hydrogels with encapsulated nanobeads (one 30-μL hydrogel per each cylindrical mold, diameter = 4.6 mm, thickness = 1.8 mm). The hydrogels were washed with PBS thrice to remove any non-encapsulated nanobeads and then gently rocked at room temperature in 1 mL of PBS buffer for photodegradation studies or PBS with 10 mM GSH for GSH-mediated release. An aliquot of the sink solution (100 μL) was removed for release measurements and replaced by 100 μL of fresh sink solution for cumulative release measurements in bulk degradation experiments. For surface erosion studies, a 100-μL aliquot of the fresh solution was added back to the sink solution, ensuring a constant sink volume and a detectable concentration of nanobeads in the sink solution. The concentration of nanobeads released at each time point was determined using fluorescence measurements (Synergy H4, BioTek Inc., Winooski, VT), and a calibration curve for the fluorescence of nanobeads as a function of concentration was used to determine the nanobead concentration in the release solution. No significant differences in the slope of the calibration curve were observed due to photobleaching associated with light-mediated degradation experiments (p = 0.36, data not shown). The cumulative release (*R*) at each time point was calculated using the following equation:

$$R_t = V_r C_r + \sum_{i=1}^{n} (V_{m_i} C_i) \qquad \ldots(S10)$$

where V_m and V_r indicate amount of sink solution used for release measurement and remaining volume of sink solution, respectively, (i.e., total volume of the sink, $V = V_r + V_m$) at each time point measurement; C is the concentration of released nanobeads obtained using fluorometry and the appropriate calibration curve; and i is the number of experiment time points. For light-mediated release studies, the expected release (~15%) was calculated based on the rate of degradation of hydrogels under similar irradiation conditions: specifically, 120-µm thick hydrogels completely degraded by ~4.5 minutes, consequently, with 10 minutes of irradiation, 267 microns of these thick hydrogel samples (~1.8 mm) and 15 % of beads were estimated to be released, assuming uniform distribution of beads throughout hydrogel samples.

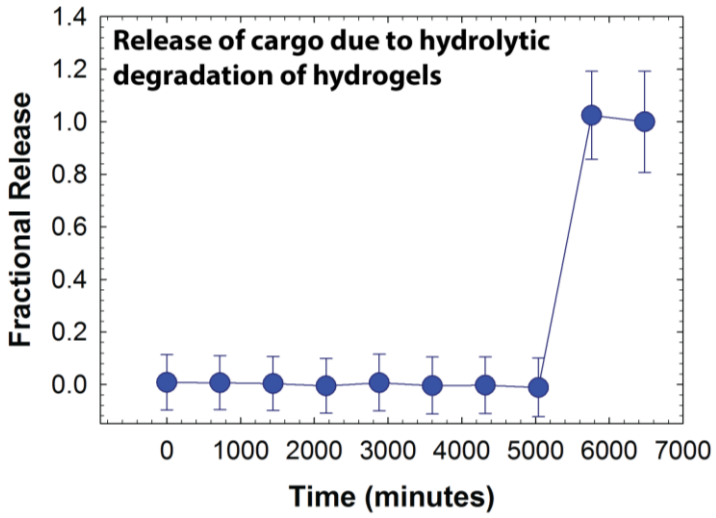

Fig. S7. Degradation-mediated release of cargo in response to hydrolytic degradation. Encapsulated nanobeads were released after 4 days (5760 minutes) upon complete dissolution of the hydrogel owing to bulk degradation by ester hydrolysis. The data shown illustrate the mean ($n \geq 5$) with error bars showing the standard error.

11. Statistical analysis

Data are presented as mean ± standard error. At a minimum three samples were averaged for each data point for all experiments. Statistical comparisons were based on analysis of variance (ANOVA), and $p < 0.05$ was considered statistically significant.

12. NMR Spectra

^{1}H NMR spectrum for synthesized compounds are shown below with relevant shifts identified.

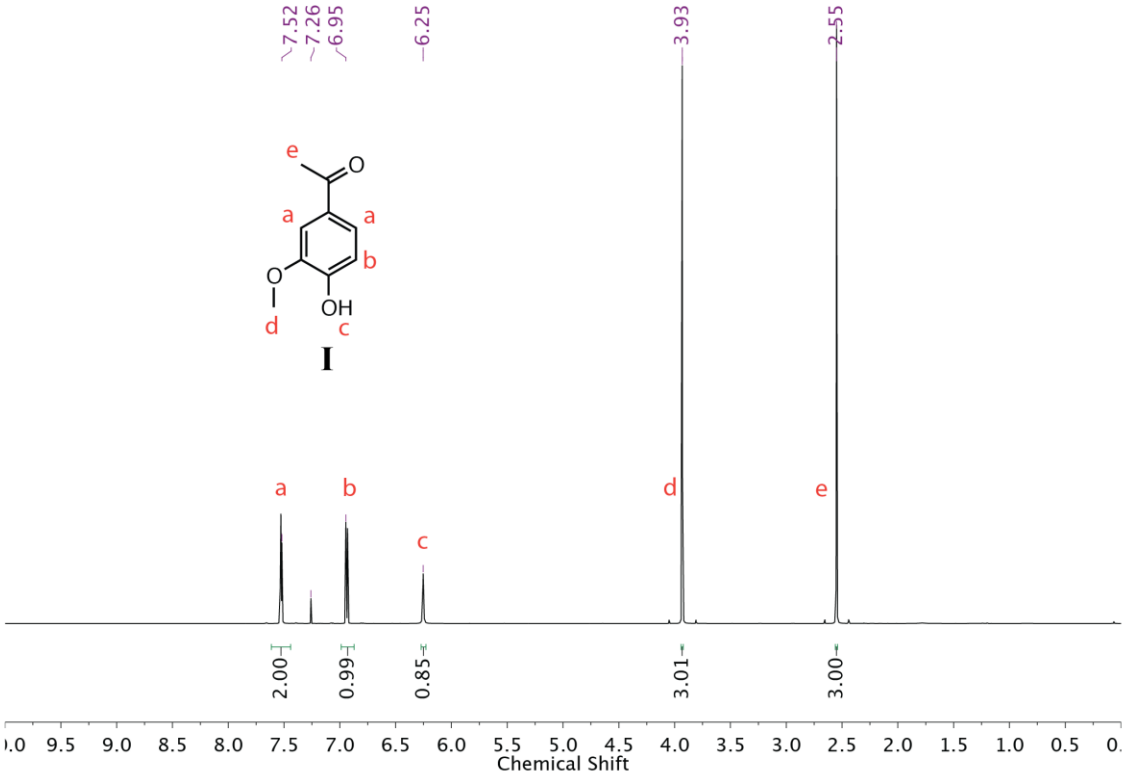
7.52
7.26
6.95
6.25
3.93
2.55
e
O
a
a
b
O
OH
d
c
I
a
b
c
d
e
2.00
0.99
0.85
3.01
3.00
Chemical Shift

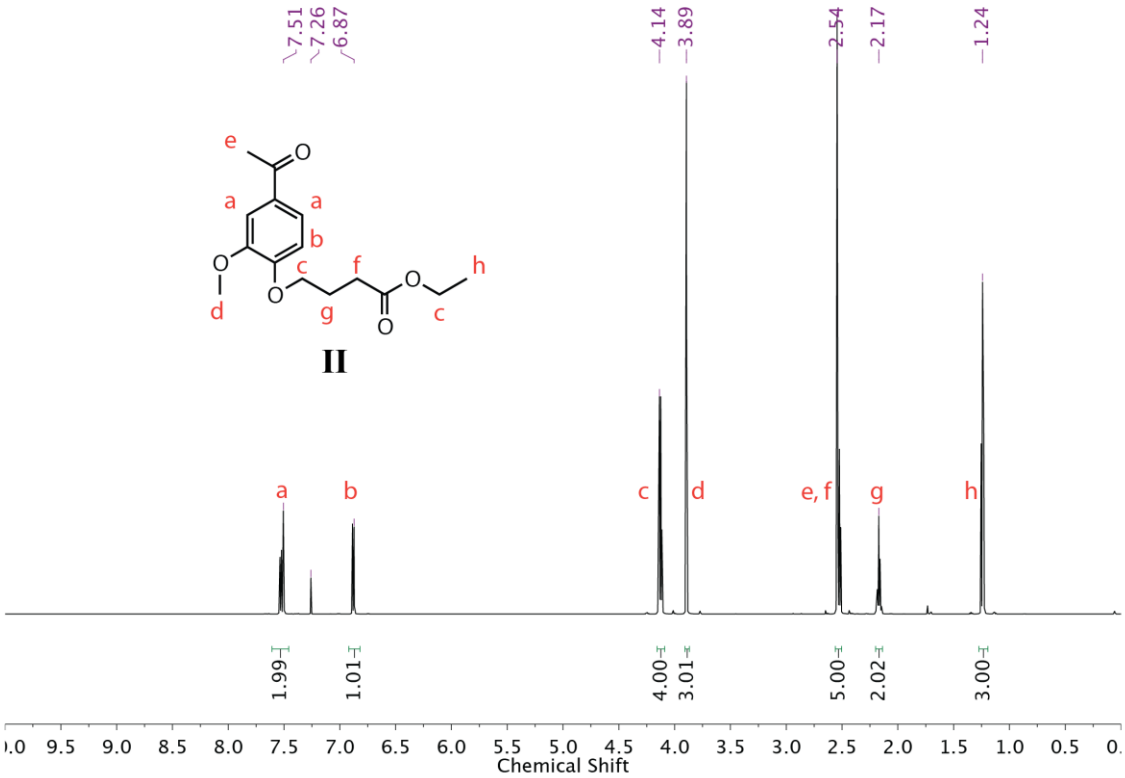
7.51
7.26
6.87
4.14
3.89
2.54
2.17
1.24
e
O
a
a
b
c
f
h
O
O
d
g
O
c
II
a
b
c
d
e, f
g
h
1.99
1.01
4.00
3.01
5.00
2.02
3.00
Chemical Shift

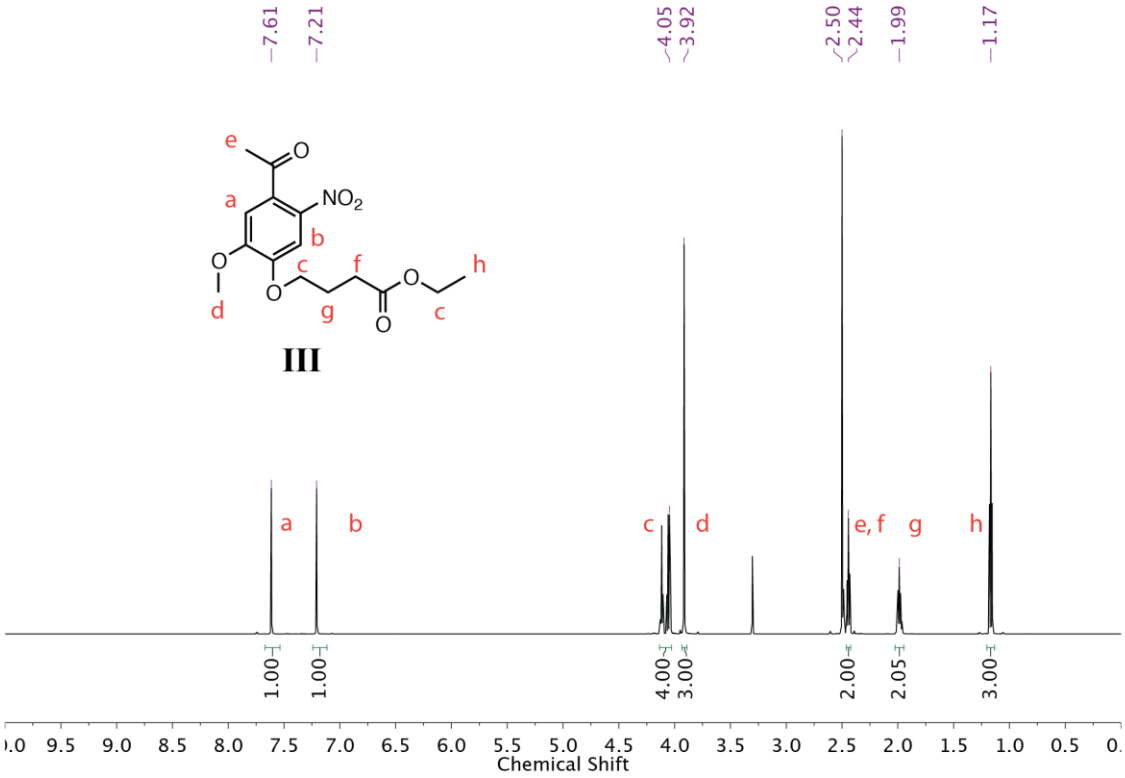
7.61
7.21
4.05
3.92
2.50
2.44
1.99
1.17
e
O
a
NO2
b
O
c
f
O
h
d
O
g
c
O
III
a
b
c
d
e, f
g
h
1.00
1.00
4.00
3.00
2.00
2.05
3.00
Chemical Shift

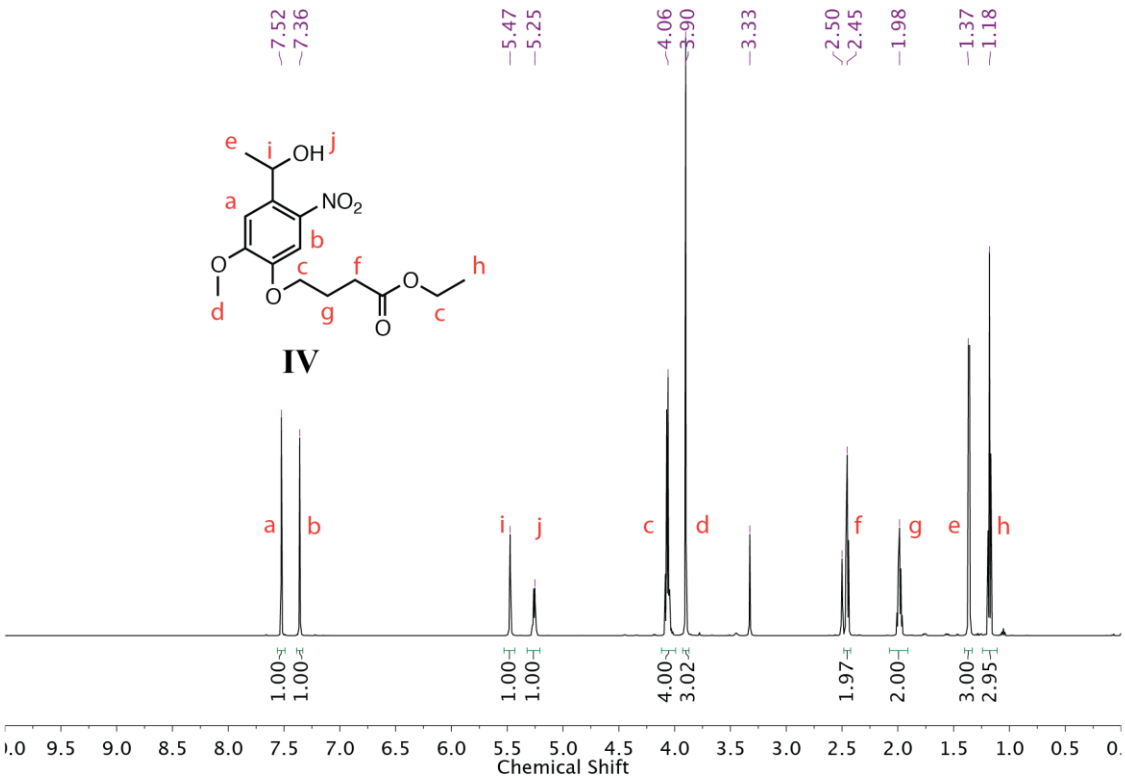
7.52
7.36
5.47
5.25
4.06
3.90
3.33
2.50
2.45
1.98
1.37
1.18
e
i
OH
j
a
NO2
b
O
c
f
O
h
d
O
g
c
O
IV
a
b
i
j
c
d
f
g
e
h
1.00
1.00
1.00
1.00
4.00
3.02
1.97
2.00
3.00
2.95
Chemical Shift

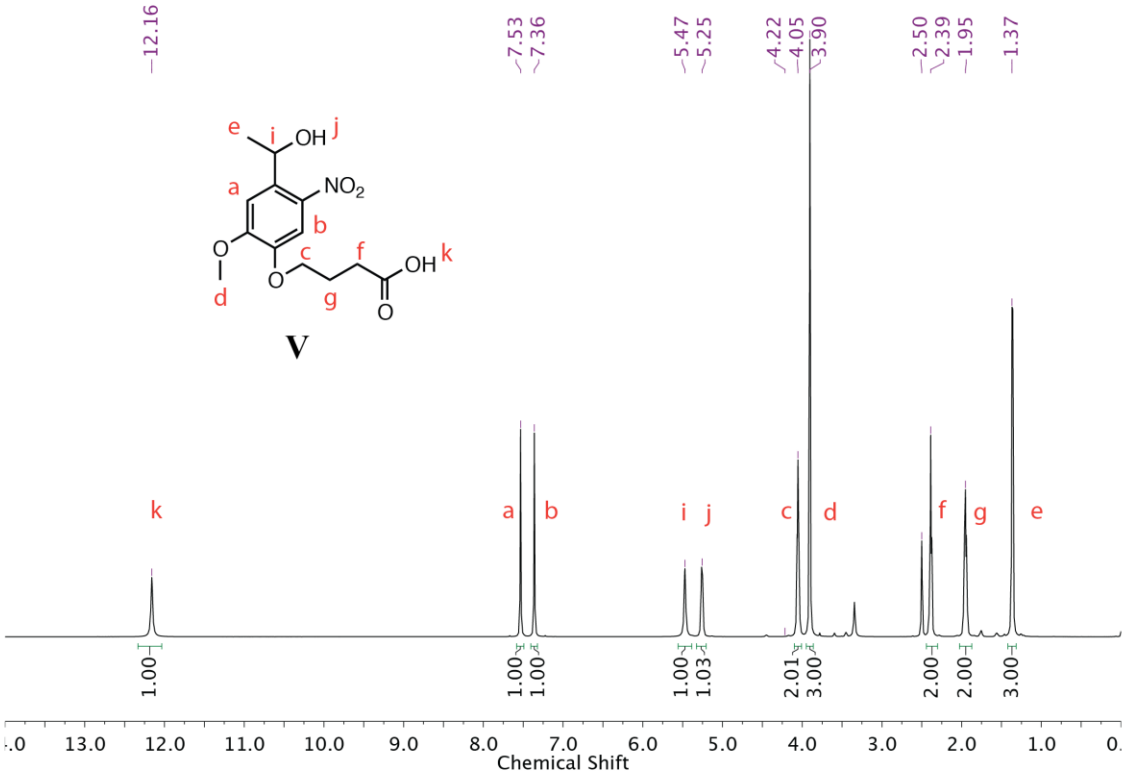
12.16
7.53
7.36
5.47
5.25
4.22
4.05
3.90
2.50
2.39
1.95
1.37
V
Chemical Shift

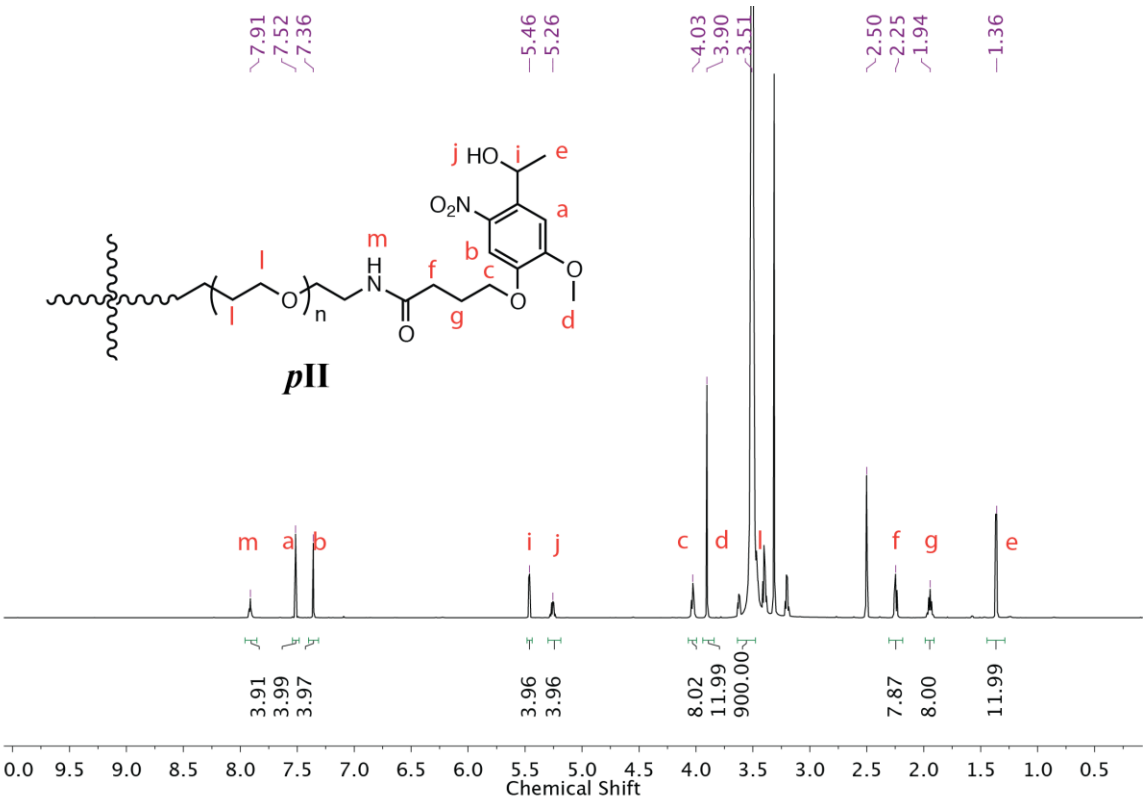
7.91
7.52
7.36
5.46
5.26
4.03
3.90
3.51
2.50
2.25
1.94
1.36
pII
Chemical Shift

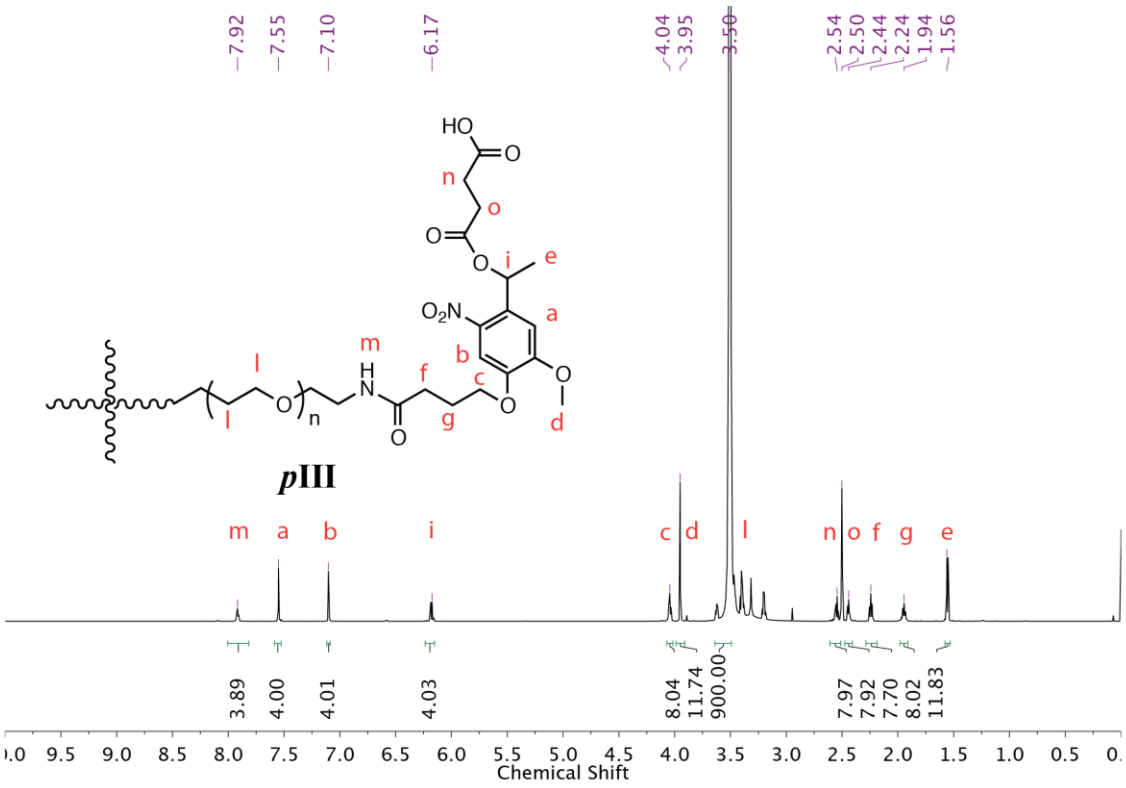
pIII
Chemical Shift

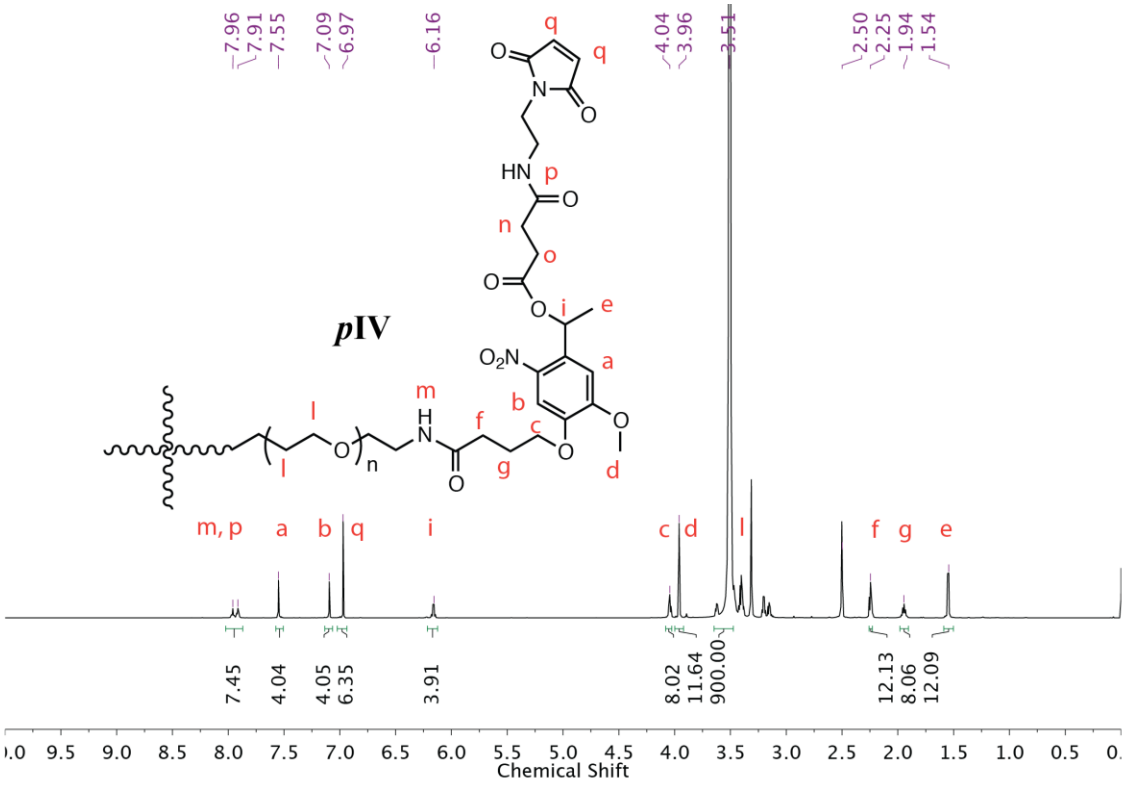
pIV
Chemical Shift

13. References

1. A. M. Kloxin, M. W. Tibbitt and K. S. Anseth, Synthesis of photodegradable hydrogels as dynamically tunable cell culture platforms, 2010, 5, 1867-1887.
2. P. M. Kharkar, A. M. Kloxin and K. L. Kiick, Dually degradable click hydrogels for controlled degradation and protein release, 2014, 2, 5511-5521.
3. S. P. Zustiak and J. B. Leach, Characterization of protein release from hydrolytically degradable poly (ethylene glycol) hydrogels, 2011, 108, 197-206.
4. P. J. Flory, *Principles of polymer chemistry*, Cornell University Press, 1953.
5. J. Brandrup and E. H. Immergut, *Polymer Handbook*, Wiley-Interscience, New York, 1975.
6. T. Canal and N. A. Peppas, J Biomed Mater Res, 1989, 23, 1183-1193.
7. L. R. G. Treloar, *The physics of rubber elasticity*, Oxford university press, 1975.